An Alternative Method to WKB Approximations and Its Applications to Cosmology & Gravitational Wave Physics

Anzhong Wang
GCAP-CASPER
Phys. Dept.
Baylor University

Peng Huanwu Center for Fundamental Theory
USTC, Hefei, China
June 30, 2023

Collaborators

Content

- Introduction
- UAA Method
- Applications
- Conclusions



(G. Cleaver) (K. Kirsten) (Q. Sheng)



(B.-F. Li) (B. Wu) (T. Zhu)

(BU Ph.D. & Postdoc, 2014-20) (BU Ph.D., 2005-09) (BU postdoc, 2013-18)

Collaborators

- Graduate Students:

(J. Marchetta)

(J. Saeed)

(R. Pan)

1. Introduction

- The 1D Schrodinger equation reads,

$$\frac{d^2\Psi(x)}{dx^2} + \frac{2m}{\hbar^2}\Big(E - V(x)\Big)\Psi(x) = 0,$$

m, E: the particle mass and total energy;
V(x): the potential

- With the WKB approximation, the wavefunction is given by

$$\Psi(x) \simeq \frac{\hbar}{\sqrt{2|p(x)|}} \exp\left[\pm\frac{i}{\hbar}\int^{x} p(x')dx'\right],$$

$$p(x) \equiv \sqrt{2m\left[E - V(x)\right]}$$

$E \mp V(x)$

1. Introduction (Cont.)

➢ The WKB approximation is valid only when

$$Q \equiv \hbar^2 \left| \frac{3p'^2}{4p^4} - \frac{p''}{2p^3} \right| \ll 1.$$

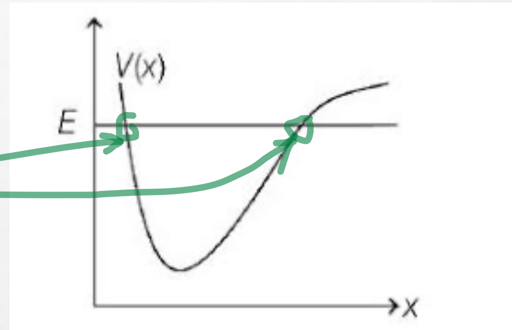

➢ The WKB condition is violated around various points:

- turning points, V(x) = E
- singular points, $V(x) = \pm\infty$, for example, the effective potential for radial motion contains a centrifugal term:

$$V_C(r) = \frac{\hbar^2 l(l+1)}{2mr^2}$$

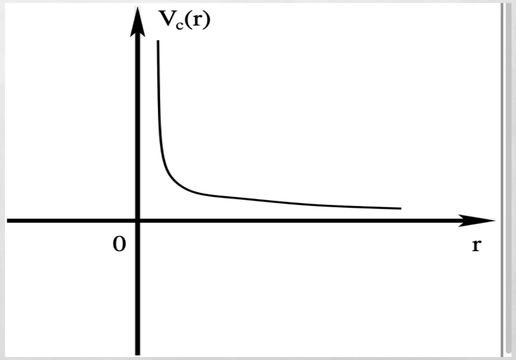

1. Introduction (Cont.)

➢ The WKB condition is violated around various points (Cont.):

- extreme points, at which we have

$$\mathcal{Q} \simeq \left|\frac{p''}{2p^3}\right| \sim \mathcal{O}(1)$$

- multiple turning points

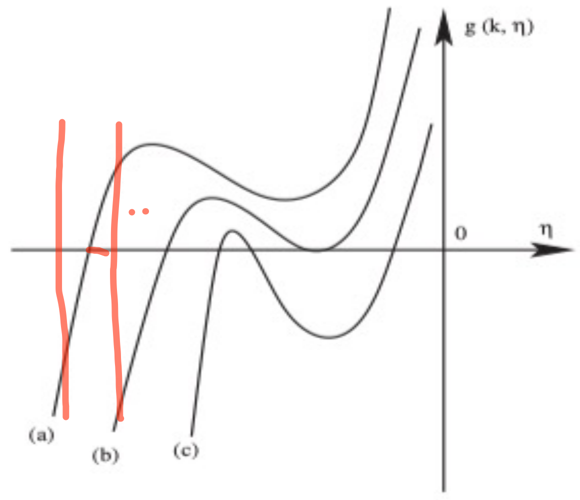

FIG. 2. The three different cases for the function $g(k, \eta)$ defined by Eq. (5.22): (a) $g(k, \eta)$ has one turning point; (b) $g(k, \eta)$ has two turning points; and (c) $g(k, \eta)$ has three turning points.

[AW, PRD82 (2010)124063]

1. Introduction (Cont.)

- When Trans-Planckian Physics is involved, the dispersion relation becomes nonlinear. Then, the WKB method is valid only when

$\lambda << L_H$

Where $\lambda = 1/k$, $L_H = 1/aH$

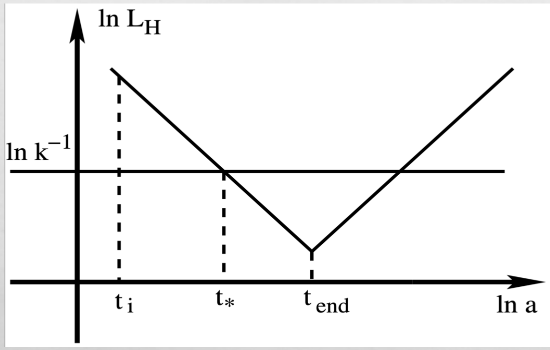

PHYSICAL REVIEW D **79,** 023514 (2009)

Trans-Planckian physics from a nonlinear dispersion relation

S. E. Jorás

Instituto de Física, Universidade Federal do Rio de Janeiro, Caixa Postal 68528, Rio de Janeiro, RJ 21941-972, Brazil

G. Marozzi

Dipartimento di Fisica, Università degli Studi di Bologna and INFN, via Irnerio 46, I-40126 Bologna, Italy

(Received 28 August 2008; published 22 January 2009)

We study a particular nonlinear dispersion relation $\omega_p(k_p)$—a series expansion in the physical wave number k_p—for modeling first-order corrections in the equation of motion of a test scalar field in a de Sitter spacetime from trans-Planckian physics in cosmology. Using both a numerical approach and a semianalytical one, we show that the WKB approximation previously adopted in the literature should be used with caution, since it holds only when the comoving wave number $k \gg aH$. We determine the amplitude and behavior of the corrections on the power spectrum for this test field. Furthermore, we consider also a more realistic model of inflation, the power-law model, using only a numerical approach to determine the corrections on the power spectrum.

DOI: 10.1103/PhysRevD.79.023514 PACS numbers: 98.80.Cq, 98.70.Vc

1. Introduction (Cont.)

(JWKB = WKB)

- In loop quantum cosmology (LQC):

QIANG WU, TAO ZHU, and ANZHONG WANG PHYS. REV. D **98,** 103528 (2018)

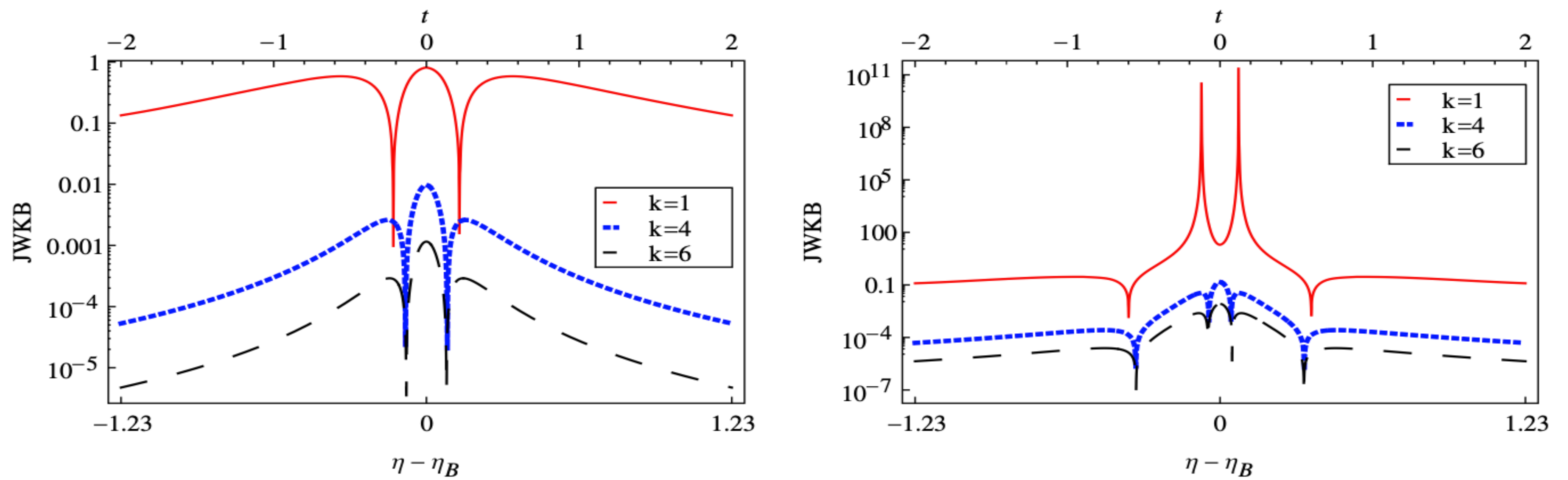

FIG. 3. The JWKB criterion is violated near the time of the bounce at $t = 0$. The left panel shows the result for the hybrid approach and the right panel shows the result for the dressed metric approach. Note that we used units where $m_{\rm Pl} = 1$ and set $a_{\rm B} = 1$ in these figures.

1. Introduction (Cont.)

- To overcome these problems, various (approximation) methods have been proposed, including the complex and uniform WKB methods [S.-H. Dong, *Wave Equations in Higher Dimensions*, Springer, Dordrecht (New York, 2011)].

- In this talk, I shall introduce another one, the so-called uniform asymptotic approximation (UAA) method, developed by Olver in 1950's – 70's:

  - F.W. J. Olver, *The Asymptotic Solution of Linear Differential Equations of the Second Order in a Domain Containing One Transition Point*, Philos. Trans. R. Soc. Math. Phys. Eng. Sci. 249 (1956) 65

  - F.W. J. Olver, *Second-Order Linear Differential Equations with Two Turning Points,* Philos. Trans. R. Soc. Math. Phys. Eng. Sci. 278 (1975) 137

  - F.W. J. Olver, *Asymptotics and Special Functions* (Wellesley, 1997)

2. The Uniform Asymptotic Approximation (UAA) Method

- The Schrodinger equation can be cast in the form,

$$\frac{d^2\mu_k(y)}{dy^2} = f(k,y)\mu_k(y)$$

In fact, all the linear second-order homogeneous ordinary differntial equations can be cast in this form.

- However, instead of the above form, we further write it as,

$$\frac{d^2\mu_k(y)}{dy^2} = \left[\lambda^2 g(y) + q(y)\right]\mu_k(y) \quad (2.1)$$

$g(y)$, $q(y)$: two unspecified functions

λ : a large positive dimensionless parameter and serves as a bookmark

2. The UAA Method (Cont.)

- Then, we expand $\mu_k(y)$ in terms of λ^{-n}

$$\mu_k(y) = \sum_{n=0}^{\infty} \frac{\mu_k^{(n)}(y)}{\lambda^n}.$$

At the end, without loss of generality, we shall set it to one, by absorbing it to $\mu_k^{(n)}(y)$. Note that the above expansion usually does not converge, and in these cases we just expand $\mu_k(y)$ to a finite order, say N, so that $\mu_k(y)$ is well approximated by the linear combination of the first N terms.

- The reason to introduce two functions, g(y) and q(y), instead of a single one, f(y), is to use this extra degree of freedom to minimize the errors, by writing them in the form

$$g = g(y, a_n), \quad q = g(y, b_n)$$

a_n, b_n: a set of parameters, which will be chosen to minimize the errors.

2. The UAA Method (Cont.)

- Then, there are ~~two~~ three major steps:
  - The Liouville Transformation
  - Minimizing the errors
  - Properly choosing $y(\xi)$

2.1 The Liouville Transformation

- The Liouville transformation:

$$U(\xi) \equiv \dot{y}^{-1/2}\mu_k, \quad \dot{y} \equiv \frac{dy}{d\xi} > 0. \qquad (2.2)$$

- Then, Eq.(2.1) takes the form,

$$\frac{d^2U(\xi)}{d\xi^2} = \left[\lambda^2(\dot{\mathbf{y}}^2\mathbf{g}) + \psi(\xi)\right]U(\xi), \qquad (2.3)$$

with

$$\psi(\xi) \equiv \dot{y}^2 q + \dot{y}^{1/2}\frac{d^2}{d\xi^2}\left(\dot{y}^{-1/2}\right) = \dot{y}^2 q - \dot{y}^{3/2}\frac{d^2}{dy^2}\left(\dot{y}^{1/2}\right) \equiv \psi(y). \qquad (2.4)$$

2.2 Minimizing the Errors

- If

$$\left|\frac{\psi(\xi)}{\lambda^2 \dot{y}^2 g}\right| \ll 1$$

we can ignore the $\psi(\xi)$ term in Eq.(2.3) to find the first-order approximate solution.

- To characterize the errors, we introduce *the error control function,*

$$F(\xi) \equiv \int^{\xi} \frac{\psi(v)}{|\dot{y}^2 g(v)|^{1/2}} dv$$

and *the associated error control function*

$$\mathscr{V}_{a,b}(F) \equiv \int_a^b \frac{|\psi(v)|}{|\dot{y}^2 g(v)|^{1/2}} dv$$

2.2 Minimizing the Errors (Cont.)

- Our goal now is to choose $\dot{y}^2 g(\xi)$ properly, so that:
  - ✓ the first-order approximate equation,

$$\frac{d^2U(\xi)}{d\xi^2} = \lambda^2 \dot{y}^2 g\, U(\xi), \quad (\psi(\xi) = 0)$$

can be solved explicitly *(often in terms of known special functions)*

  - ✓ the first-order approximation can be as close to the exact solution as possible. This requirement can be fulfilled by minimizing the error control function

$$\frac{\partial F(\xi, a_n, b_n)}{\partial a_n} = 0, \quad \frac{\partial F(\xi, a_n, b_n)}{\partial b_n} = 0 \quad \Leftarrow g = g(\xi, a_n), \quad q = q(\xi, b_n),$$

2.2 Minimizing the Errors (Cont.)

- ✓ the requirment,

$$\mathscr{V}_{\alpha,\beta}(F) < \infty, \quad \forall \alpha, \beta \in (\alpha_1, \alpha_2),$$

where (α_1, α_2) is the interval we are interested in, which (one-to-one) correaspónds to (a_1, a_2) of y, and can be finite or infinite.

2.3 Choices of $y(\xi)$

- The choice of $y(\xi)$ sensitively depends on the properties of the functions $g(y)$ and $q(y)$ near their *poles* (singularities) and *turning points* (roots of $g(y) = 0$).

- In particular, depending on the number and nature of the turning points, the choices of will be different.

- Examples of Turning Points

  - Zero Turning Point:

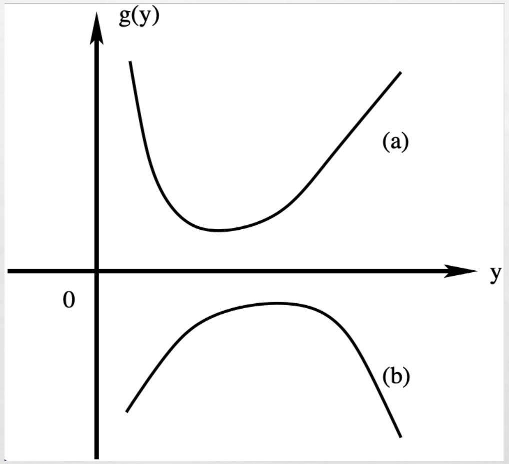

(Zero Turning Point without Poles)

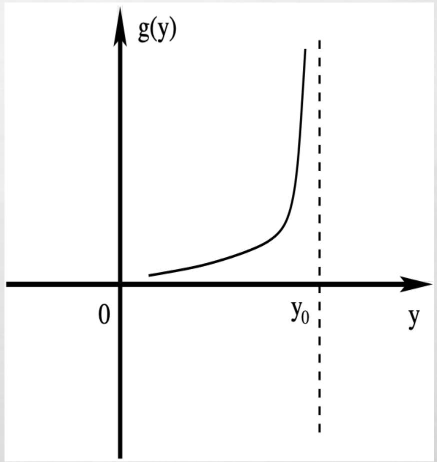

(Zero Turning Point with a Pole at y_0)

2.3 Choices of $y(\xi)$ (Cont.)

- One Turning Point:

  * Note that we shall consider Cases (b) & (d) as double turning points, and only consider Cases (a) and (c) as a single turning point.

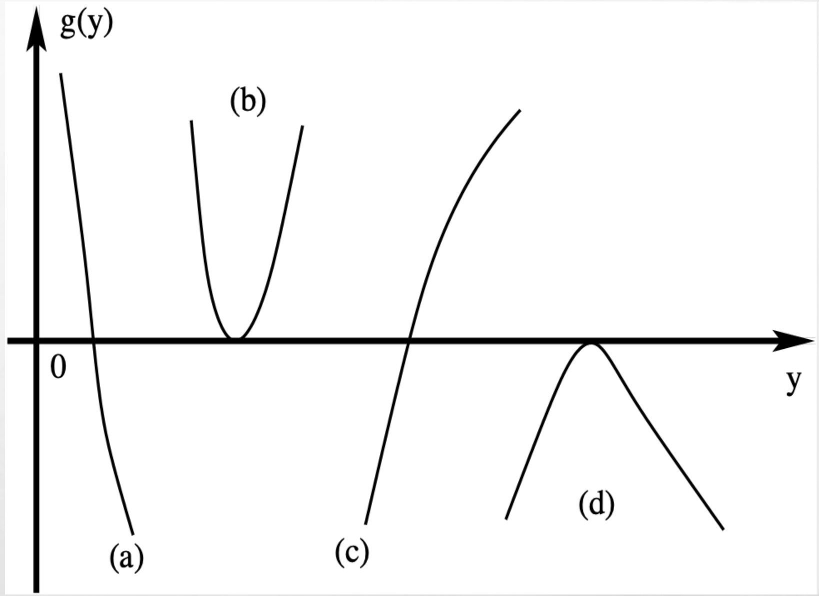

(One Turning Point)

2.3 Choices of $y(\xi)$ (Cont.)

- Two Turning Points:

In general, we have three different cases:

- ✓ both are real and different;
- ✓ both are real and equal (double roots);
- ✓ both are complex roots. Since $g(y)$ is real, in this case they must be complex conjugate $y_1 = y_2^*$.
- ✓ We shall treat these three cases all together.

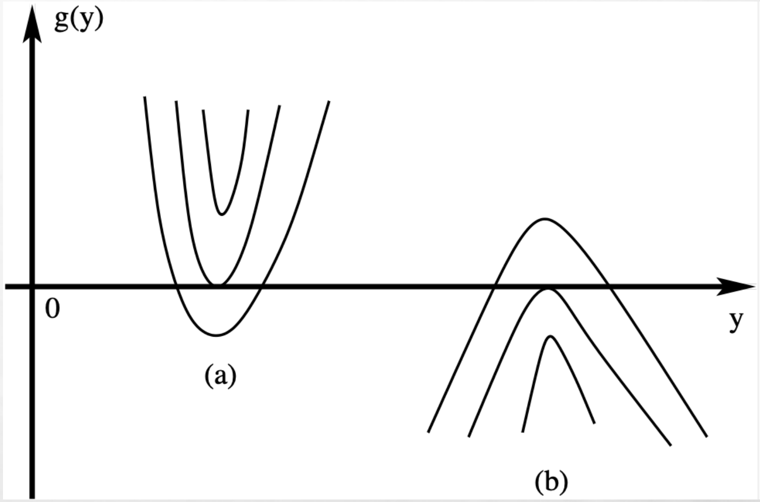

(Two Turning Points)

2.3 Choices of y(ξ) (Cont.)

- For each case, we choose [T. Zhu, AW, G. Cleaver, K. Kirsten, Q. Sheng, *PRD*89 (2014) 043507]

$$\dot{y}^2 g = \begin{cases} \text{sgn}(g), & \text{zero turning point,} \\ \xi, & \text{one turning point,} \\ \text{sgn}(g)\left(\xi_0^2 - \xi^2\right), & \text{two turning points,} \end{cases} \qquad \text{sgn}(g) = \begin{cases} +1, & g > 0, \\ -1, & g < 0. \end{cases}$$

$$\xi_0^2 = \pm\frac{2}{\pi}\left|\int_{y_1}^{y_2} \sqrt{g(y)}dy\right|$$

"+": $y_{1,2}$ are real; "-": $y_{1,2}$ are complex

$y_{1,2}$: the two turning points (roots) of $y(y) = 0$.

2.4 Approximate Solutions

- For such choices, it can be seen that y is a monotonically increasing function of ξ , so that the map between y and ξ are one-to-one.

- For the cases with more than two turning points, see, for example, J.-L. Zhang, *Extended Airy function and differential equations with N-turning points, Appl. Math. Mechanics*, 12 (1991) 907.

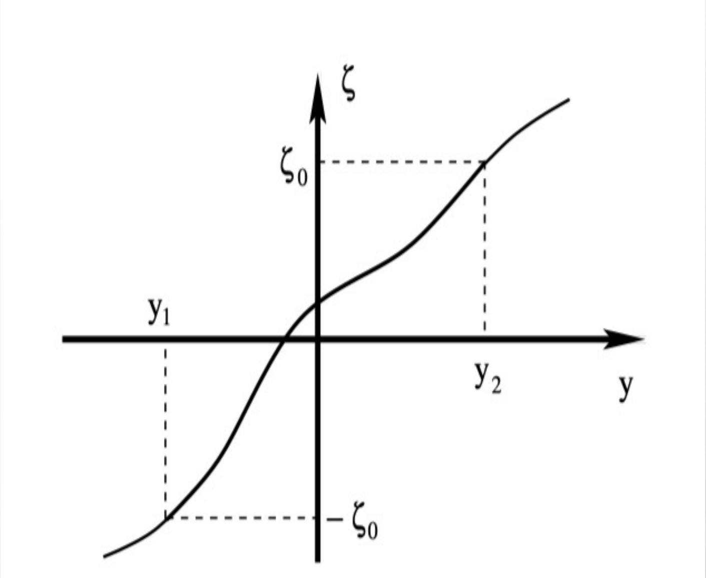

2.4 Approximate Solutions (Cont.)

- Then, the first-order approximate solutions of the equation,

$$\frac{d^2U(\xi)}{d\xi^2} = \lambda^2 \dot{y}^2 g\, U(\xi), \quad (\psi(\xi) = 0)$$

are given by [T. Zhu, AW, G. Cleaver, K. Kirsten, Q. Sheng, *PRD*89 (2014) 043507]

$$U(\xi) = \begin{cases} a_+ e^{\lambda\sqrt{\mathrm{sgn(g)}}\,\xi} + a_- e^{-\lambda\sqrt{\mathrm{sgn(g)}}\,\xi}, & \text{zero turning point} \\ a_+ \mathrm{Ai}\left(\lambda^{2/3}\xi\right) + a_- \mathrm{Bi}\left(\lambda^{2/3}\xi\right), & \text{one turning point} \\ a_+ W\left(\frac{1}{2}\xi_0^2, \sqrt{2\lambda}\,\xi\right) + a_- W\left(\frac{1}{2}\xi_0^2, -\sqrt{2\lambda}\,\xi\right), & \text{two turning points} \end{cases}$$

$a_\pm$: constants;
Ai, Bi: Airy functions;
W: modified parabolic cylindrical function

2.4 Approximate Solutions (Cont.)

- High order solutions can be obtained by recursion relations [Zhu, AW, Cleaver, Kirstein, and Sheng, *PRD*89 (2014) 043507; T. Zhu, AW, K. Kirsten, G. Cleaver, Q. Shgeng, PRD93 (2016) 123525].

- For example, for the one-turning point case, we have

$$U(\xi) = \alpha_k \left[\mathrm{Ai}(\lambda^{2/3}\xi) \sum_{s=0}^{n} \frac{A_s(\xi)}{\lambda^{2s}} + \frac{\mathrm{Ai}'(\lambda^{2/3}\xi)}{\lambda^{4/3}} \sum_{s=0}^{n-1} \frac{B_s(\xi)}{\lambda^{2s}} + \epsilon_3^{(2n+1)} \right]$$
$$+\beta_k \left[\mathrm{Bi}(\lambda^{2/3}\xi) \sum_{s=0}^{n} \frac{A_s(\xi)}{\lambda^{2s}} + \frac{\mathrm{Bi}'(\lambda^{2/3}\xi)}{\lambda^{4/3}} \sum_{s=0}^{n-1} \frac{B_s(\xi)}{\lambda^{2s}} + \epsilon_4^{(2n+1)} \right],$$

2.4 Approximate Solutions (Cont.)

$$A_{s+1}(\xi) = -\frac{1}{2}B_s'(\xi) + \frac{1}{2}\int \psi(v)B_s(v)dv,$$

$$B_s = \begin{cases} \frac{1}{2\xi^{1/2}} \int_0^{\xi} \{\psi(v)A_s(v) - A_s''(v)\} \frac{dv}{v^{1/2}}, & \xi > 0, \\ \frac{1}{2(-\xi)^{1/2}} \int_{\xi}^{0} \{\psi(v)A_s(v) - A_s''(v)\} \frac{dv}{(-v)^{1/2}}, & \xi < 0, \end{cases}$$

$$A_0(\lambda, \xi) = 1$$

$\epsilon_{(3,4)}^{(2n+1)}$: errors, which is related to the associated error control function, $\mathcal{V}_{\xi_1,\xi_2}$, and

2.4 Approximate Solutions (Cont.)

$$\left|\epsilon_j(\lambda,\xi)\right|, \quad \frac{1}{2\lambda}\left|\epsilon_j'(\lambda,\xi)\right| \le \begin{cases} \exp\left|\frac{\mathscr{V}_{a_j,y}(F)}{2\lambda}\right| - 1, & \mathrm{sgn}(g) = +1, \\ \exp\left|\frac{\mathscr{V}_{a,y}(F)}{\lambda}\right| - 1, & \mathrm{sgn}(g) = -1, \end{cases}$$

$a \in [a_1, a_2],\ \epsilon_j' \equiv \partial\epsilon_j/\partial\xi.$

- From the above expression we can see that, to minimize the errors, we need to minimize the error control function F(y). In particular, when

$$F(y) = 0 \quad \Rightarrow \quad \left|\epsilon_j(\lambda,\xi)\right|, \quad \frac{1}{2\lambda}\left|\epsilon_j'(\lambda,\xi)\right| = 0,$$

which corresponds to the exact solution! In general we cannot have F(y) = 0. But it does show the importance to properly choose $g(y, a_n)$ and $q(y, b_n)$, so that the error control function F(y) is minimized.

- This is the key to construct successfully approximate solutions of μ_k.

3. Applications

3.1 Quantum Mechanics (QM)

- In QM, exact solutions of the Schrodinger equation

$$\frac{d^2\Psi(x)}{dx^2} + \frac{2m}{\hbar^2}\Big(E - V(x)\Big)\Psi(x) = 0,$$

are known for several potentials V(x) [S.-H. Dong, *Wave Equations in Higher Dimensions* (Springer, New York, 2011)], as given in the Table.

- In the following, let us compare WKB and Our methods for these particular cases [B.-F. Li, T. Zhu, AW, Universe 6 (2020) 90; arXiv:1920.09675]

Potentials	$V(x)$
Hydrogen	$-\frac{e^2}{x} + \frac{\hbar^2 l(l+1)}{2mx^2}$
Harmonic oscillator	$\frac{1}{2}m\omega^2x^2 + \frac{\hbar^2 l(l+1)}{2mx^2}$
Morse potential	$v_0e^{-2\alpha x} + v_1e^{-\alpha x}$
Pöschl-Teller (PT)	$\frac{v_0}{\cosh^2(\alpha x)}$
Eckart	$\frac{v_0}{\sinh^2(\alpha x)} + \frac{v_1}{\tanh(\alpha x)}$

[Potentials for which exact solutions are known]

3.1.1 Hydrogen Atoms

- In this case, the potential is given by

$$V(x) = -\frac{e^2}{x} + \frac{\hbar^2 l(l+1)}{2mx^2},$$

m, e: the electron mass and charge; l: the angular momentum number

- The corresponding exact solutions of the Schrodinger equation are known, from which the energy eigenvalues are given by [S.-H. Dong, S.-H. *Wave Equations in Higher Dimensions* (Springer, New York, 2011)]

$$E_n^{\text{Exact}} = -\frac{me^4}{2\hbar^2(n+l+1)^2}.$$

3.1.1 Hydrogen Atoms (Cont.)

- The WKB method yields

$$E_n^{\mathrm{WKB}} = -\frac{me^4}{2\hbar^2(n + 1/2 + \sqrt{l(l+1)})^2} \neq E_n^{\mathrm{Exact}}.$$

- To fix this problem, Langer [R. Langer, The Asymptotic Solutions of Linear Ordinary Differential Equations with Reference to the Stokes Phenomenon, Bull. Am. Math. Soc. 40 (1934) 545] introduced the following replacement

$$l(l+1) \quad \Rightarrow \quad (l+1/2)^2$$

in the Schrodinger equation, without any (physical) justification.

3.1.1 Hydrogen Atoms (Cont.)

- On the other hand, the potential diverges at $x = 0$. So, in the framework of the UAA method, in order to have the error control function $F(x)$ be finite near this pole, $q(x)$ must be chosen as

$$q(x) = -\frac{1}{4x^2},$$

which is nothing but the Langer's modification!

- With such a choice, $g(y) = 0$ now has two real and different roots

$$x_{1,2} = -\frac{e^2}{2E} \pm \frac{\sqrt{m^2E^4 + mE(l+1/2)^2\hbar^2}}{2mE}$$

3.1.1 Hydrogen Atoms (Cont.)

- Then, the energy eigenvalues are given by

$$E_n^{\mathrm{UAA}} = -\frac{me^4}{2\hbar^2(n+l+1)^2} = E_n^{\mathrm{Exact}}.$$

3.1.2 Harmonic Oscillators

- The potential for the harmonic oscillator in D-dimensions is given by

$$V(x) = \frac{1}{2}m^2\omega^2x^2 + \frac{\hbar^2}{2mx^2}\left(l\,(D+l-2) + \frac{1}{4}(D-1)(D-3)\right).$$

- The exact solution of the Schrodinger equation leads to [S.-H. Dong, S.-H. *Wave Equations in Higher Dimensions* (Springer, New York, 2011)],

$$E_n^{\text{Exact}} = \left(2n + l + \frac{D}{2}\right)\hbar\omega.$$

- The WKB method gives

$$E_n^{\text{WKB}} = \left(2n + \sqrt{l\,(D+l-2) + \frac{(D-1)(D-3)}{4} + 1}\right)\hbar\omega.$$

Which is also different from the exact one.

3.1.2 Harmonic Oscillators (Cont.)

- On the other hand, in the framework of the UAA method, the finite requirement of the error control function F(y) leads to the unique choice,

$$q(x) = -\frac{1}{4x^2},$$

for which we find that

$$E_n^{\text{UAA}} = \left(2n + l + \frac{D}{2}\right)\hbar\omega = E_n^{\text{Exact}}$$

3.1.3 Poschl-Teller (PT) Potential

- The PT potential is given by

$$V(x) = \frac{v_0}{\cosh^2(\alpha x)}, \qquad v_0, \alpha: \text{ constants.}$$

- The exact solution of the Schrodinger equation leads to [S.-H. Dong, S.-H. *Wave Equations in Higher Dimensions* (Springer, New York, 2011)],

$$E_n^{\text{Exact}} = v_0 - \frac{\alpha^2\hbar^2}{4m}\left[2n^2 + 2n + 1 - (2n+1)\sqrt{1 - \frac{8mv_0}{\alpha^2\hbar^2}}\right].$$

- The WKB method gives

$$E_n^{\text{WKB}} = v_0 - \frac{\alpha^2\hbar^2}{4m}\left[\frac{(2n+1)^2}{2} - (2n+1)\sqrt{-\frac{8mv_0}{\alpha^2\hbar^2}}\right].$$

3.1.3 PT Potential (Cont.)

- On the other hand, in the framework of the UAA method, we choose

$$q(x) = \frac{\alpha^2}{4\cosh^2(\alpha x)},$$

which leads precisely to

$$E_n^{\mathrm{UAA}} = E_n^{\mathrm{Exact}}.$$

3.1.4 Other Potentials

- For other potentials (listed in the previous Table), by properly choosing q(y), the UAA method always yields [B.-F. Li, T. Zhu, AW, Universe 6 (2020) 90; arXiv:1920.09675],

$$E_n^{\mathrm{UAA}} = E_n^{\mathrm{Exact}}.$$

Potentials	$V(x)$	$q(x)$	$E_n^{\mathrm{WKB}} = E_n^{\mathrm{Exact}}$	$E_n^{\mathrm{UAA}} = E_n^{\mathrm{Exact}}$
Hydrogen	$-\frac{e^2}{x} + \frac{\hbar^2 l(l+1)}{2mx^2}$	$-\frac{1}{4x^2}$	×	√
Harmonic oscillator	$\frac{1}{2}m\omega^2 x^2 + \frac{\hbar^2 l(l+1)}{2mx^2}$	$-\frac{1}{4x^2}$	×	√
Morse potential	$v_0 e^{-2\alpha x} + v_1 e^{-\alpha x}$	0	√	√
Pöschl-Teller (PT)	$\frac{v_0}{\cosh^2(\alpha x)}$	$\frac{\alpha^2}{4\cosh^2(\alpha x)}$	×	√
Eckart	$\frac{v_0}{\sinh^2(\alpha x)} + \frac{v_1}{\tanh(\alpha x)}$	$-\frac{\alpha^2}{4\sinh^2(\alpha x)}$	×	√

- For other applications of the UAA method to QM, see B.-F. Li, T. Zhu, AW, Universe 6 (2020) 90 [arXiv:1920.09675].

3.2 Cosmology

- The first application of the UAA method gravity physics was by S. Habib, et al. in 2002 with a single turing point to the first-order approximation, precisely 46 years after Olver first studied this case [F.W.J. Olver, Philos. Trans.Roy. Soc. London A249 (1956) 65].

VOLUME 89, NUMBER 28 PHYSICAL REVIEW LETTERS 31 DECEMBER 2002

The Inflationary Perturbation Spectrum

Salman Habib,[1] Katrin Heitmann,[1] Gerard Jungman,[1] and Carmen Molina-París[2]

[1]*Theoretical Division, MS B285, Los Alamos National Laboratory, Los Alamos, New Mexico 87545*

[2]*Mathematics Institute, University of Warwick, Coventry CV4 7AL, United Kingdom*

(Received 23 August 2002; published 27 December 2002)

Motivated by the prospect of testing inflation from precision cosmic microwave background observations, we present analytic results for scalar and tensor perturbations in single-field inflation models, based on the application of uniform approximations. This technique is systematically improvable, possesses controlled error bounds, and does not rely on assuming the slow-roll parameters to be constant. We provide closed form expressions for the power spectra and the corresponding scalar and tensor spectral indices.

3.2 Cosmology (Cont.)

- Later, the same authors generalized their studies to high-order approximaitns [S. Habib, *et al.*, PRD70 (2004) 083507; D71 (2005) 043518].

- In 2008, Lorenz *et al.* applied the method to k-inflaiton and obtained the power spectra up to the first-order approximation [L. Lorenz, et al., PRD78 (2008) 083513].

- In 2009, Yamamoto *et al.* applied the method to calculate the power spectra of cosmological perturbations in the HL gravity [K. Yamanoto, et al., PRD80 (2009) 063514].

- Note that up to this moment (2009) all the applications were restricted to the one-turning point case.

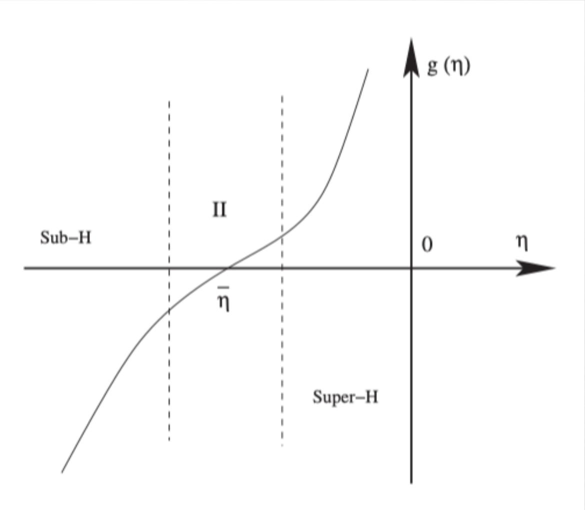

[AW, PRD82 (2010) 124063]

3.2 Cosmology (Cont.)

- But the problem is really a three-turning-point problem. In order to calculate the power spectra of cosmological perturbations correctly, one needs to generalize the one-turning-point case to three-turning-point one [AW, *PR*D82 (2010) 124063; Y. Huang, AW, Q. Wu, JCAP10 (2012) 010].

- Very fortunately, in 2013 Dr. Tao Zhu joined Baylor as a postdoc to work with Jerry, Klaus, Tim & me, through CASPER, and we immediately proposed to work on the above problem.

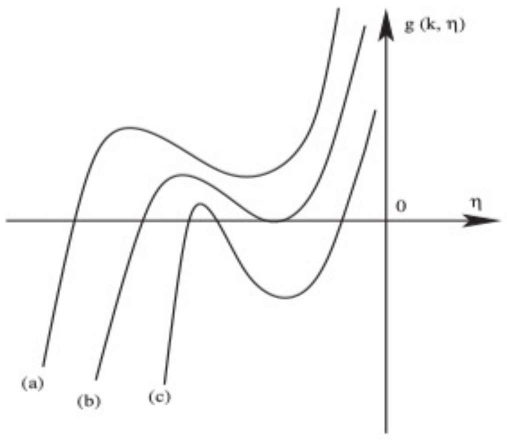

FIG. 2. The three different cases for the function $g(k, \eta)$ defined by Eq. (5.22): (a) $g(k, \eta)$ has one turning point; (b) $g(k, \eta)$ has two turning points; and (c) $g(k, \eta)$ has three turning points.

[AW, PRD82 (2010)124063]

- In that year, we worked out the first-order approximation to the case with two singular and three turning points to the first-order approximation [T. Zhu, AW, G. Cleaver, K. Kirsten, Q. Sheng, *IJMPA*29 (2014) 1450142; *PRD*89 (2014) 043507].

3.2 Cosmology (Cont.)

- Later, we generalized our studies to high-order approximations:
  - Case (a) [T. Zhu, AW, G. Cleaver, K. Kirsten, Q. Sheng, PRD90 (2014) 063503]
  - Cases (b) & (c) [T. Zhu, AW, K. Kirsten, G. Cleaver, Q. Shgeng, PRD93 (2016) 123525]

- In particular, we found that to the third-order approximation, the upper bound of errors is no larger that 0.15%, which are sufficiently accurate for the current and forthcoming cosmological observations [Y. Akrami, et al., Planck Collaboration, *Planck 2018 results: I. Overview and the cosmological legacy of Planck*, A&A 641 (2020) A1]

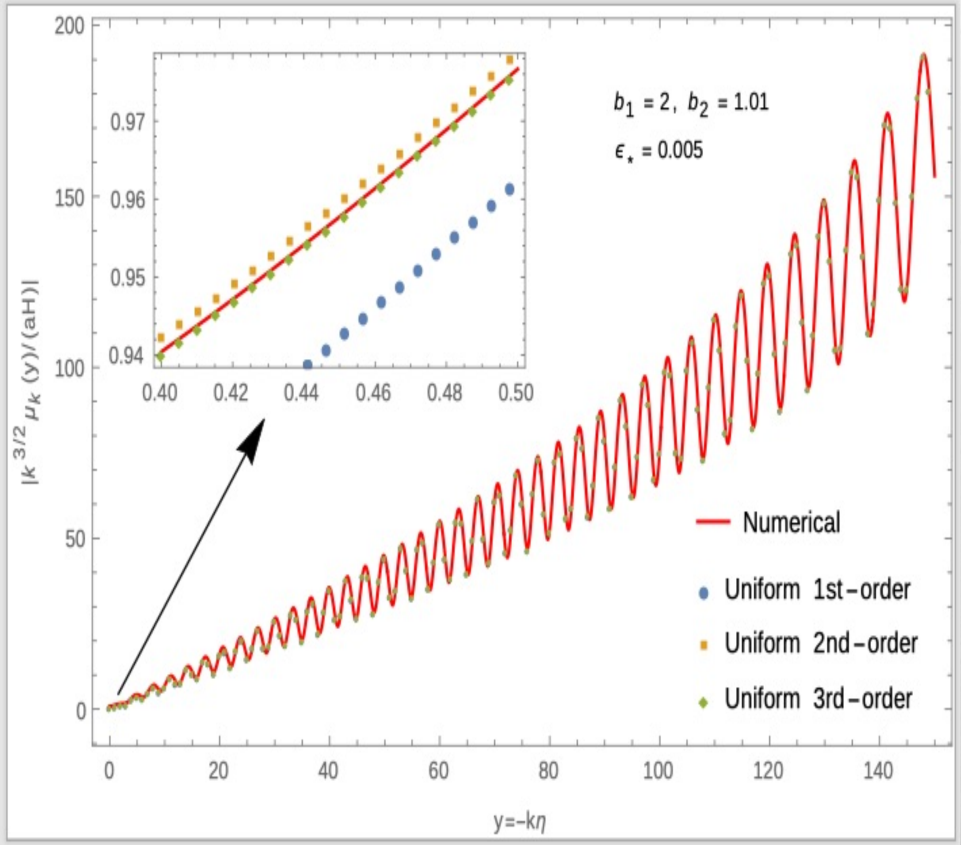

3.2 Cosmology (Cont.)

- Power spectrum of cosmological scalar perturbations in *Deforemd Algebra Approach* [M. Bojowald, et al., 2008; T. Cailleteau et al., 2012; A. Barrau, et al., 2015]:
  - Equation:

$$\mu_k'' + \left(\omega k^2 - \frac{z_S''}{z_S}\right)\mu_k = 0, \quad z_s \equiv \frac{\phi'}{H},$$

$$\omega \equiv 1 - \frac{2\rho}{\rho_c} = \begin{cases} > 0, & \rho \le \frac{\rho_c}{2}, \\ = 0, & \rho = \frac{\rho_c}{2}, \\ < 0, & \rho \ge \frac{\rho_c}{2}. \end{cases}$$

  - Silent point:

$$\rho = \frac{1}{2}\rho_c.$$

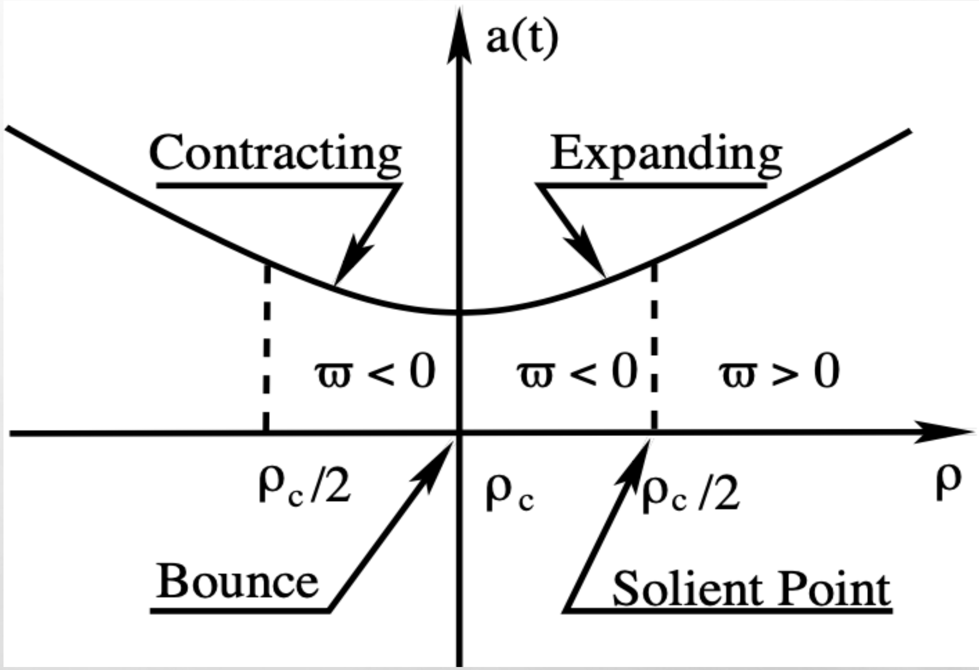

3.2 Cosmology (Cont.)

- Imposing *the Minkowski vacuum initial conditions at remote past of the quantum bounce*, it was found that the power spectra of both scalar and tensor perturbations are inconsistent with observatins [B. Bolliet et al, PRD93 (2016) 124011]:

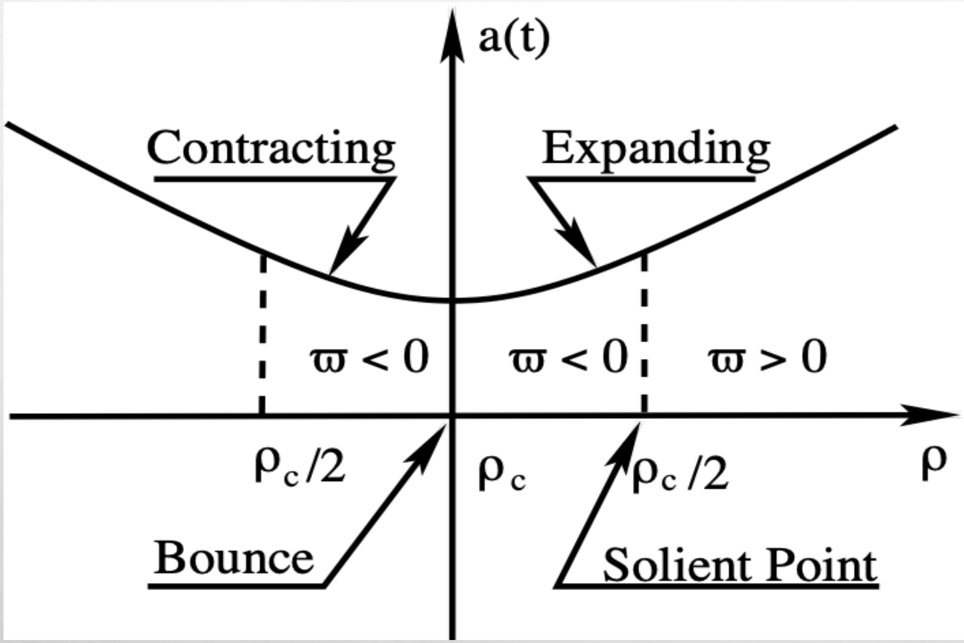

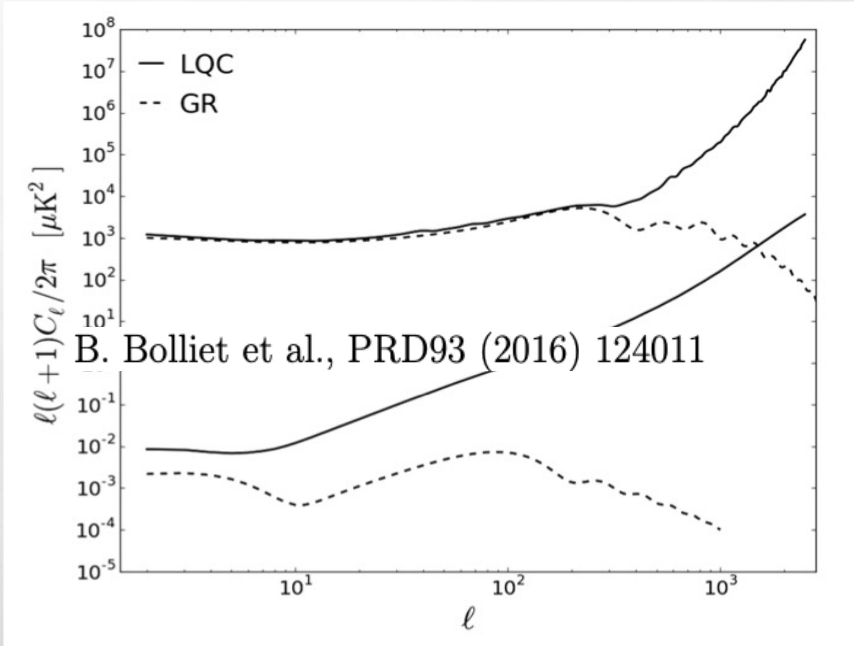

3.2 Cosmology (Cont.)

➢ In the framework of the UAA method, to make the error control function

$$F(\xi) \equiv \int \frac{\psi(\xi)}{|\dot{y}^2 g|^{1/2}} d\xi$$

be finite, we must choose

$$q(t) = -\frac{1}{4k^2 t^2}$$

➢ Then, g(t) has only one turning point. So, to the first-order approximaiton, it is the linear combination of the Airy functions.

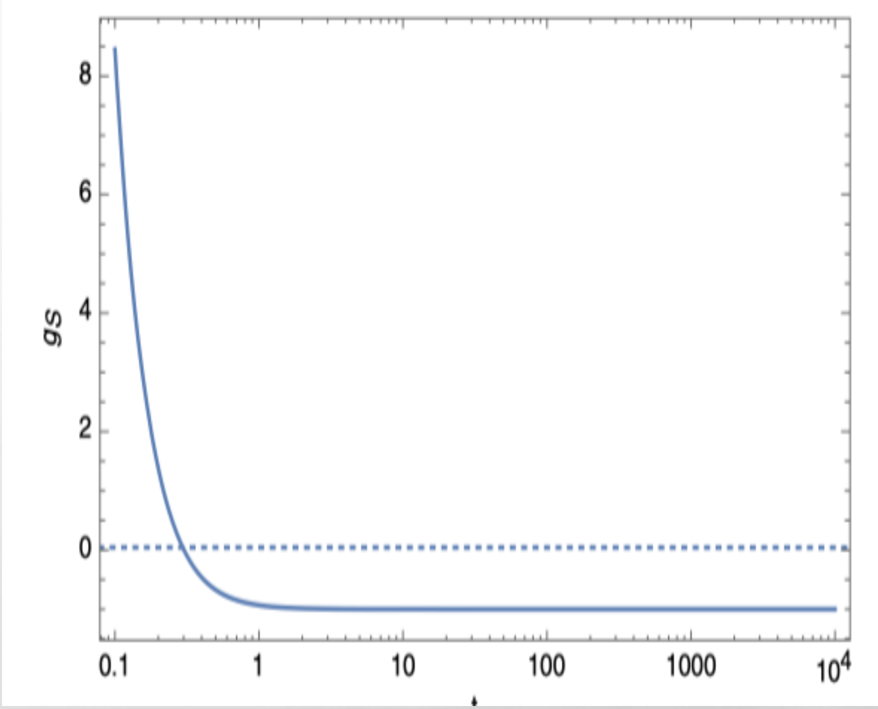

3.2 Cosmology (Cont.)

- From the figure, it can be seen that even to the first-order approximation, the numerical (exact) solution can be described well by the analytical approximate solution.

- With the general analytical solutions, we find that the unique consistent initial conditions at the silent point are

$$a_k = \sqrt{\frac{\pi}{2k}}, \qquad b_k = -i\sqrt{\frac{\pi}{2k}},$$

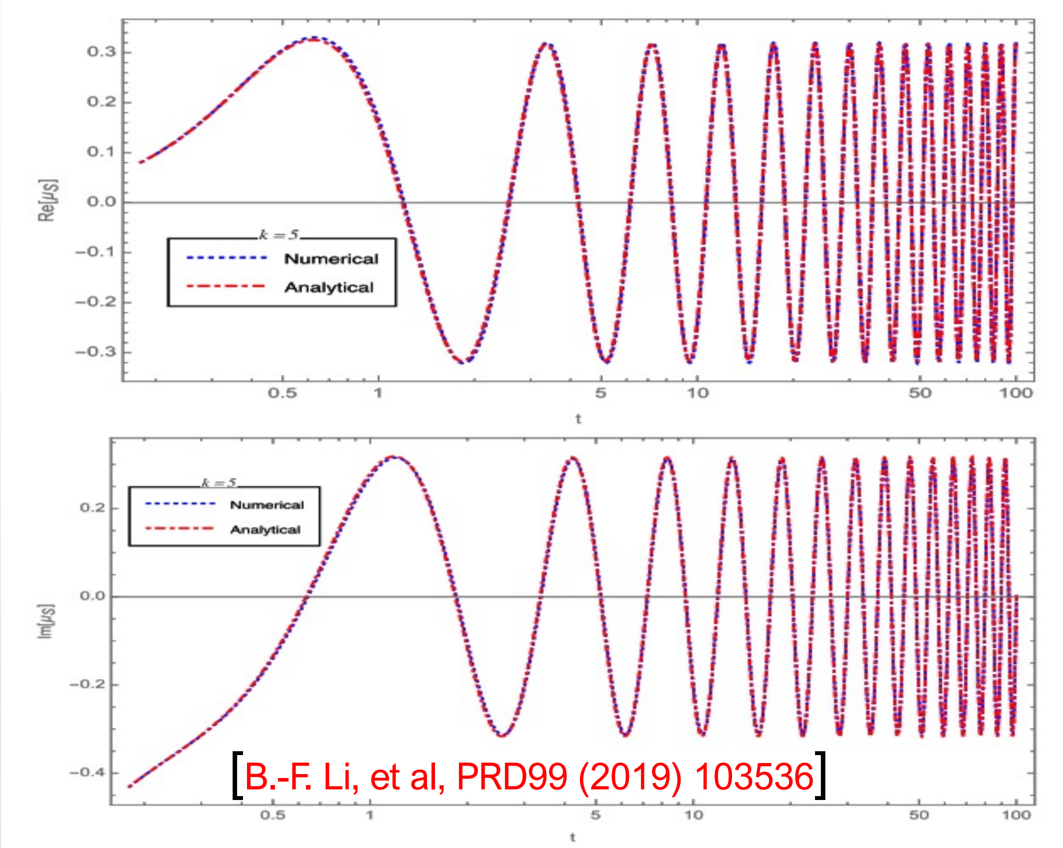

[B.-F. Li, et al, PRD99 (2019) 103536]

3.2 Cosmology (Cont.)

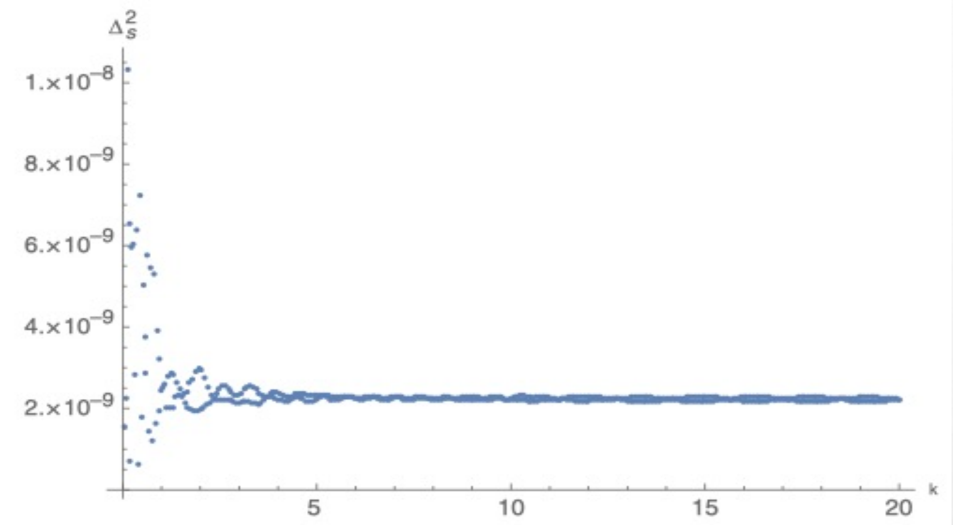

[Consistent with Observations]

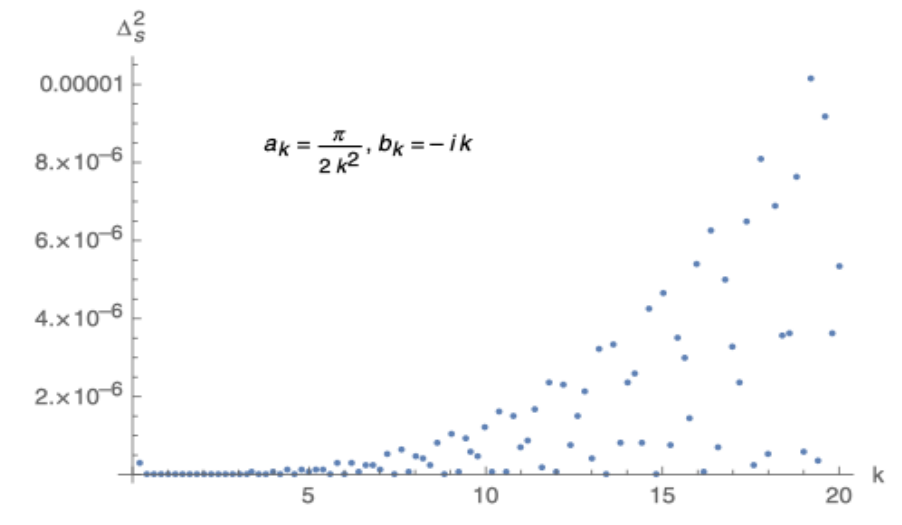

[Inconsistent with Observations]

- It important to note that the above results can be obtained only after the general analytical solutitons are known, so we are able to explore the whole initial data space.

3.3 Applications to Gravitaitonal Waves

- Recewntly, using this method, we have also calculated:
  - ✓ QNMs of black holes, arXiv:1902.09675
  - ✓ the gravitaitonal waveforms in parity-violating gravity, arXiv:1911.01580; arXiv:2211.16825
  - ✓ Gravitational Waveforms in Spatially Covariant Gravity, arXiv:2211.04711

3.3 Applications to Gravitaitonal Waves (Cont.)

Parity-Violated Gravity：

$$\tilde{h}''_A + (2+\nu_A)\mathcal{H}\tilde{h}'_A + (1+\mu_A)k^2\tilde{h}_A = 0, \quad (4.3)$$

where a prime denotes a derivative with respect to the conformal time τ. The deviations from that in GR are quantified by the quantities ν_A and μ_A, which are given by

$$\nu_A = \frac{\rho_A k(c_1\mathcal{H} - c_1')/(a\mathcal{H}M_{\rm PV})}{1-\rho_A k c_1/(aM_{\rm PV})}, \quad (4.4)$$

$$\mu_A = \frac{\rho_A k(c_1 - c_2)/(aM_{\rm PV})}{1-\rho_A k c_1/(aM_{\rm PV})}. \quad (4.5)$$

The quantity ν_A describes the modification of the friction term, and μ_A describes the modification of the dispersion relation of GWs. In parity-violating gravities, the former induces the amplitude birefringence effect of GWs, while the latter induces the velocity birefringence of GWs. In the

PHYSICAL REVIEW D **101,** 043528 (2020)

Polarized primordial gravitational waves in the ghost-free parity-violating gravity

Jin Qiao,[1,2,†] Tao Zhu,[1,2,‡] Wen Zhao,[3,4,*] and Anzhong Wang[5,§]

[1]*Institute for theoretical physics and Cosmology, Zhejiang University of Technology, Hangzhou, 310032, China*
[2]*United center for gravitational wave physics (UCGWP), Zhejiang University of Technology, Hangzhou, 310032, China*
[3]*CAS Key Laboratory for Research in Galaxies and Cosmology, Department of Astronomy, University of Science and Technology of China, Hefei 230026, China*
[4]*School of Astronomy and Space Sciences, University of Science and Technology of China, Hefei, 230026, China*
[5]*GCAP-CASPER, Physics Department, Baylor University, Waco, Texas 76798-7316, USA*

(Received 8 November 2019; accepted 6 February 2020; published 20 February 2020)

The tests of parity symmetry in the gravitational interaction is an attractive issue in gravitational-wave astronomy. In the general theories of gravity with parity violation, one of the fundamental results is that primordial gravitational waves (PGWs) produced during slow-roll inflation is circularly polarized. In this article, we investigate the polarization of PGWs in the recently proposed ghost-free parity-violating gravity, which generalizes Chern-Simons gravity by including higher derivatives of the coupling scalar field. For this purpose, we first construct the approximate analytical solution to the mode function of the PGWs during slow-roll inflation by using the uniform asymptotic approximation. With the approximate solution, we explicitly calculate the power spectrum and the corresponding circular polarization of the PGWs analytically, and find that the contributions of the higher derivatives of the coupling scalar field to the circular polarization are of the same order of magnitude as that of Chern-Simons gravity. The degree of circular polarization of PGWs is suppressed by the energy scale of parity violation in gravity, which is unlikely to be detected using only the two-point statistics of future cosmic microwave background data.

3.3 Applications to Gravitaitonal Waves (Cont.)

Using UAA, first found the mode functiopns

- Solid blue: GR
- Green: CS theory
- Darker Yellow: PV theory

QIAO, ZHU, ZHAO, and WANG PHYS. REV. D **101,** 043528 (2020)

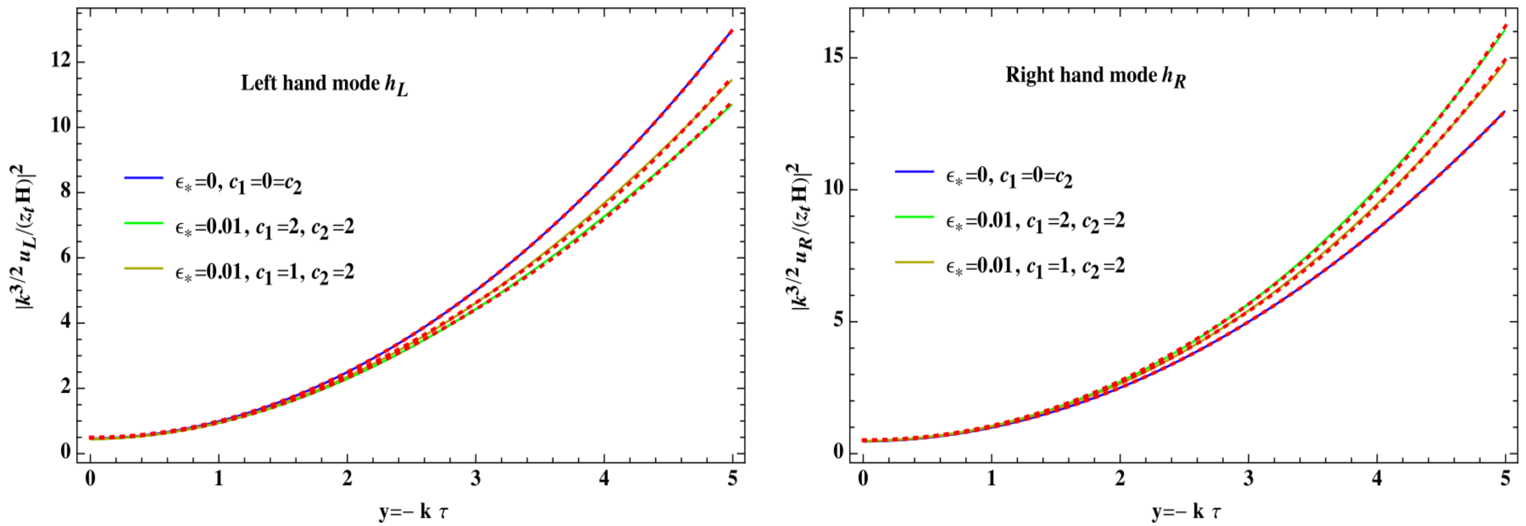

FIG. 1. Uniform asymptotic approximate solutions of mode functions $|k^{3/2}u_A/(z_tH)|^2$ (solid curves) and the corresponding numerical solutions (dotted curves). The left and right panels show the solutions of the left-hand and right-hand modes, respectively. In each panel, the solid blue, green, and darker yellow curves correspond to the solutions for general relativity, Chern-Simons theory, and ghost-free parity-violating gravities, respectively. The numerical solution associated with each analytical solution is shown by the red dotted curves.

3.3 Applications to Gravitaitonal Waves (Cont.)

Then, using our analytical solutions,

- we explicitly calculated both the power spectra for the two polarization modes
- we showed that in the presence of parity violation the power spectra of PGWs are slightly modified.
- the circular polarization generated in the ghost-free parity-violating theory of gravity is quite small, suppressed by the energy scale of parity violation of the theory, and it would be difficult to detect using only the power spectra of future CMB data.
- However, previous calculations in Chern-Simons gravity showed that parity-violation signatures in the bispectrum could be large enough to be detected in the future CMB observations [N. Bartolo and G. Orlando, JCAP 07 (2017) 034]

3.3 Applications to Gravitaitonal Waves (Cont.)

- In particular, it was found that the tensor-tensor-scalar bispectra for each polarization state can be peaked in the squeezed limit by setting the level of parity violation during inflation.

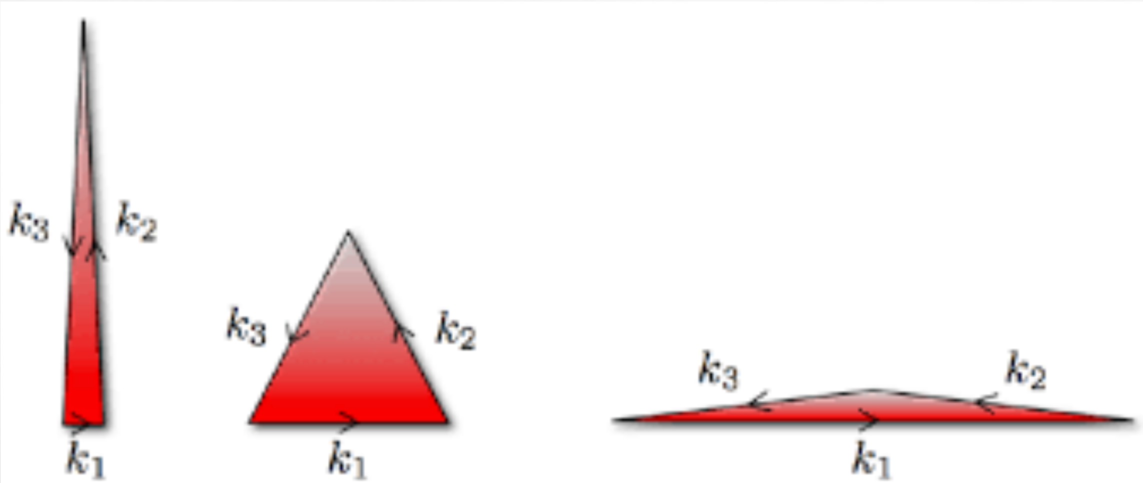

- Therefore, it would be interesting to further explore whether the ghost-free parity-violating theory of gravity could lead to any parity-violation signatures in non-Gaussianity of PGWs.

3.4 Applications to Other Fields

- After developing the general formulas, we have applied the UAA method to study analytically the power spectra of cosmological perturbations and non-Gaussianities in various theories of gravity, including

  - ✓ k-inflation, arXiv:1407.8011
  - ✓ Loop quantum cosmology, ; arXiv:1503.06761; arXiv:1508.03239; arXiv:1510.03855; arXiv:1812.11191
  - ✓ Einstein-scalar-Gauss-Bonnet cosmology, arXiv:1707.08020
  - ✓ Cosmology in Effective Theories of Gravity, arXiv:1811.03216; arXiv:1811.12612; arXiv:1907.13108
  - ✓ Cosmology in 4D EGB Gravity, arXiv:2212.08253

4. Conclusions & Challenges

4.1 Conclusions

- We have sucessfully applied the UAA method to various problems in several fields of physics, including:
  - ✓ the accurate calculations of power spectra of cosmological perturbations when quantum effects are taken into acocunt, which were done only numerically previously
  - ✓ gravitational waveforms in modified theories of gravity
  - ✓ QNMs of black holes
  - ✓ Energy eigenvalues in QM
- We expect that such analytical analysis will provide much deeper and thorough understanding of the physics involved.

4.1 Conclusions (Cont.)

- One advantage of the UAA method is to allow us to estimate the upper bound of errors, and more important to minimize the errors,

$$\frac{\partial F(\xi, a_n, b_n)}{\partial a_n} = 0, \quad \frac{\partial F(\xi, a_n, b_n)}{\partial b_n} = 0 \qquad \Leftarrow g = g(\xi, a_n), \quad q = q(\xi, b_n),$$

- provided that

$$\mathscr{V}_{\alpha,\beta}(F) < \infty, \quad \forall \alpha, \beta \in (\alpha_1, \alpha_2)$$

4.2 Challenges

- When we study the QNMs of black holes in modified theories of gravity, the linearized equations are normally coupled ODEs, for example,
  - ✓ in the Einstein-scalar-Gauss-Bonnet theory [D. Langlois, K. Noui, H. Roussille, arXiv:2204.04107]:

$$\frac{\mathrm{d}\hat{Y}}{\mathrm{d}r_*} \equiv n(r)\frac{\mathrm{d}\hat{Y}}{\mathrm{d}r} = \begin{pmatrix} i\omega\Psi n & 1 \\ V-\omega^2 n^2\Gamma & i\omega\Psi n \end{pmatrix}\hat{Y}\,.$$

  - ✓ in scalar-tensor gravity [O.J. Tattersall, P. Ferreira, Phys. Rev. D99 (2019) 104082]:

$$\frac{d^2\Psi}{dr_*^2} + [\omega^2 - f(r)V_Z(r)]\Psi = \frac{G_{4\phi}}{G_4} S_\varphi(\varphi, \varphi')$$

$$\frac{d^2\varphi}{dr_*^2} + [\omega^2 - f(r)V_S(r,\mu^2)]\varphi = 0,$$

↩

4.2 Challenges (Cont.)

- Another challenging question is the cosmological perturbations of LQC in the deformed algebra approach,

$$\mu_S''(\eta) + \omega_k^2 \mu_S(\eta) = 0,$$

$$\omega_k^2 \equiv \Omega(\eta) k^2 - \frac{z_S''(\eta)}{z_S(\eta)},$$

$$\Omega(\eta) \equiv 1 - \frac{2\rho(t)}{\rho_c},$$

$$z_S(\eta) \equiv a\frac{\phi'}{\mathcal{H}} = a\frac{\dot{\phi}}{H},$$

where $\Omega(\eta)$ changes signs at $\rho = \rho_c/2$. This is similar to **the Tricomi problem,**

$$\frac{\partial^2 u}{\partial y^2} + y\frac{\partial^2 u}{\partial x^2} = 0$$

in the (x, y)-plane, which leads to the change of the type of the equation.

- So far, no details have been worked out for any of the above problems.

Thank you !!!

Any question?